







## RESEARCH ARTICLE

# Using camera traps to monitor cyclic vole populations

Eivind Flittie Kleiven<sup>1\*</sup> , Pedro Guilherme Nicolau<sup>2\*</sup> , Sigrunn Holbek Sørbye<sup>2</sup> , Jon Aars<sup>3</sup> , Nigel Gilles Yoccoz<sup>1</sup>  & Rolf Anker Ims<sup>1</sup> 

<sup>1</sup>Department of Arctic and Marine Biology, Faculty of Biosciences, Fisheries and Economics, UiT The Arctic University of Norway, N-9037, Tromsø, Norway

<sup>2</sup>Department of Mathematics and Statistics, Faculty of Science, UiT The Arctic University of Norway, N-9037, Tromsø, Norway

<sup>3</sup>Norwegian Polar Institute, Fram Centre, Tromsø 9296, Norway

## Keywords

Camera trap, index-calibration regression, inverse prediction, population monitoring, Rodents

## Correspondence

Eivind Flittie Kleiven, Department of Arctic and Marine Biology, Faculty of Biosciences, Fisheries and Economics, UiT The Arctic University of Norway, N-9037 Tromsø, Norway. Tel: +47 77 64 44 91; E-mail: ekleiven@gmail.com

and

Pedro Guilherme Nicolau, Department of Mathematics and Statistics, Faculty of Science, UiT The Arctic University of Norway, N-9037 Tromsø, Norway. Tel: +47 452 56 019; E-mail: pedrognicolau@gmail.com

## Funding Information

This work is a contribution from COAT (Climate-ecological Observatory for Arctic Tundra) supported by the RCN (project nr. 245638), COAT Tools supported by UiT, and COAT Tools+ supported by Tromsø Research Foundation.

\*These authors have contributed equally.

Editor: Marcus Rowcliffe

Associate Editor: Francesco Rovero

Received: 6 May 2022; Revised: 19 October 2022; Accepted: 21 October 2022

doi: 10.1002/rse2.317

## Introduction

During the last decade, the use of camera traps has increased drastically in animal ecology as this provides a non-invasive and cost-efficient alternative to traditional census methods (Wearn & Glover-Kapfer, 2019). In studies of mammals, the use of camera traps has so far largely

## Abstract

Camera traps have become popular labor-efficient and non-invasive tools to study animal populations. The use of camera trap methods has largely focused on large animals and/or animals with identifiable features, with less attention being paid to small mammals, including rodents. Here we investigate the suitability of camera-trap-based abundance indices to monitor population dynamics in two species of voles with key functions in boreal and Arctic ecosystems, known for their high-amplitude population cycles. The targeted species—gray-sided vole (*Myodes rufocanus*) and tundra vole (*Microtus oeconomus*)—differ with respect to habitat use and spatial-social organization, which allow us to assess whether such species traits influence the accuracy of the abundance indices. For both species, multiple live-trapping grids yielding capture-mark-recapture (CMR) abundance estimates were matched with single tunnel-based camera traps (CT) continuously recording passing animals. The sampling encompassed 3 years with contrasting abundances and phases of the population cycles. We used linear regressions to calibrate CT indices, based on species-specific photo counts over different time windows, as a function of CMR-abundance estimates. We then performed inverse regression to predict CMR abundances from CT indices and assess prediction accuracy. We found that CT indices (for windows maximizing goodness-of-fit of the calibration models) predicted adequately the CMR-based estimates for the gray-sided vole, but performed poorly for the tundra vole. However, spatially aggregating CT indices over nearby camera traps enabled reliable abundance indices also for the tundra vole. Such species differences imply that the design of camera trap studies of rodent population dynamics should be adapted to the species in focus, and adequate spatial replication must be considered. Overall, tunnel-based camera traps yield much more temporally resolved abundance metrics than alternative methods, with a large potential for revealing new aspects of the multi-annual population cycles of voles and other small mammal species they interact with.

focused on large-sized species (Burton et al., 2015). Nonetheless, smaller-sized rodents represent the most abundant and specious order of mammals (Wilson & Reeder, 2005). Many rodent species are cryptic, and hence resource-demanding, or otherwise difficult to study by means of conventional methods. Hence, camera traps specifically adapted to study small rodents may advance

our ability to investigate their ecology (Rendall et al., 2014). Studying the population dynamics of small rodents is important for several reasons (Krebs, 2013). Many rodent species pose risks to humans as vectors of zoonoses (Capizzi et al., 2014; Meerburg, Singleton, & Kijlstra, 2009) or by damaging crops (Andreassen et al., 2021; Meerburg, Singleton, & Leirs, 2009). Moreover, voles and lemmings exert key ecosystem functions, especially in northern biomes where they exhibit multi-annual population cycles (Ims & Fuglei, 2005). Therefore, accurate monitoring of boreal and Arctic small rodent populations is fundamental to studies of ecosystem dynamics (Boonstra et al., 2016; Legagneux et al., 2014) and to the successful conservation of endangered species that are directly (Ims et al., 2017) or indirectly affected by their population dynamics (Henden et al., 2021; Marolla et al., 2019). Many boreal and Arctic rodent monitoring programs are still based on kill-traps (snap-traps), providing counts as indices of abundance (Cornulier et al., 2013; Ehrich et al., 2019; Hörnfeldt et al., 2005; Kleiven et al., 2018; Korpela et al., 2013; Turchin et al., 2000). However, kill-trapping is fraught with both ethical issues (Powell & Proulx, 2003) and questionable assumptions regarding sampling errors (Hanski et al., 1994). Live-trap-based, capture-mark-recapture (CMR) monitoring is less invasive and allows to account for sampling errors (Krebs et al., 2011). However, live trapping requires much effort from qualified personnel and is therefore rarely sufficiently long-term and spatially extensive to support monitoring programs. In addition, several species display very low trappability in live traps and are thus inadequately monitored by capture-recapture methods (Boonstra & Krebs, 1978; Jensen et al., 1993). In general, existing monitoring programs of rodent populations are logistically limited in terms of their coarse temporal resolution. In northern ecosystems, such monitoring is usually restricted to two trapping sessions per year (Cornulier et al., 2013). This implies an important limitation due to the multi-voltine life histories and the fast population dynamics of voles and lemmings. Camera traps may potentially resolve such constraints by providing means for spatially extensive and continuous year-round monitoring, even in climatically harsh and remote boreal and Arctic regions (Möller et al., 2021; Soininen et al., 2015).

Camera traps are today most commonly used to analyze presence-absence dynamics (i.e. occupancy probability) (Bailey et al., 2014; MacKenzie et al., 2002). However, presence-absence is a less informative population state variable than abundance, especially when density-dependent population regulatory mechanisms are of concern. Hence, the use of camera traps to estimate abundance is increasing. Most of these studies have however focused on marked (or otherwise distinguishable)

individuals (Gilbert et al., 2021; Palencia et al., 2021). For many species, such as small rodents, it is not feasible to either mark or distinguish individuals by clues that are visible *in camera* trap images. Moreover, design constraints make presence-absence-based abundance estimators less applicable in the case of unmarked small mammals.

If the aim is to study population dynamics, for instance by means of time series analyses (Barraquand et al., 2017; Cornulier et al., 2013; Stenseth, 1999), simple indices of abundance can be used if there is a proportionate relationship between true abundance and the abundance index (Gilbert et al., 2021; Hanski et al., 1994; Lambin et al., 2000; Yoccoz et al., 2001). Counts of motion-triggered photos appear to be a promising abundance index for large- to medium-sized mammals (Palmer et al., 2018). Recent studies suggest that this may also be the case for some small rodent species (Parsons et al., 2021; Villette et al., 2015). However, as of yet, such camera-based abundance indices have not been validated for rodent species that exhibit multi-annual population cycles, for instance, boreal and Arctic voles. Furthermore, previous works have been limited in scope and have not assessed the uncertainty associated with using camera trap indices to estimate population abundance. A potential challenge in the case of such population dynamics is that there may be density- and/or cyclic phase-dependent aspects of their performance (*sensu* Stenseth (1999)) that may influence the reliability of camera trap (CT) indices.

Proper calibration of CT-based abundance indices as a function of CMR-based abundance estimates is challenging. Generally, calibration consists of modeling the measurable exposure variable (e.g., a population index) as a function of a ground-truthing variable that typically is assumed to be measured accurately (e.g., a population state variable measured without error). Once a calibration function is established, it can be used in inverse regression to predict the state variable for a given value of the exposure variable (Eisenhart, 1939). The goodness of the fit of the regression may be assessed using the ordinary coefficient of determination ( $R^2$ ). In most ecological studies, the true state of a population is not known and must be estimated with some error, for instance, based on CMR trapping. As the error of the population state estimate (i.e., the ground-truth variable) may not be negligible, this becomes a more difficult calibration problem because the uncertainty of the true abundance can bias the estimation of the population state (Gopalaswamy et al., 2015). Thus, it is important to assess the accuracy of prediction after establishing a calibration function (Diefenbach et al., 1994), to ensure high precision of the abundance predictions, which can sometimes be too low (Jennelle et al., 2002). Furthermore, CT-based abundance

indices have been criticized for not being generalizable to other species or sampling sites (Jennelle et al., 2002). It is, therefore, important to investigate potential differences in the performance of the abundance index for different species, i.e., to assess the out-of-sample predictive ability of the index-calibration models.

In this study, we assess the suitability of CT-based abundance indices for studying population dynamics of the gray-sided vole (*Myodes rufocanus*) and the tundra vole (*Microtus oeconomus*). Both species are renowned for their multi-annual cycles (Cornulier et al., 2013; Hansen et al., 1999; Turchin et al., 2000) and key roles in boreal and sub-arctic ecosystems (Boonstra et al., 2016; Ims & Fuglei, 2005). The two vole species are also known to differ profoundly in their habitat use and spatial-social organization (Bondrup-Nielsen & Ims, 1990; Ims, 1987a), which provides a case for assessing whether such species-specific traits influence CT-based abundance indices (CT indices). For both species, we used time series of spatio-temporally matched CT indices and CMR estimates, spanning a wide range of abundances and different phases of the population cycle. We followed a two-step calibration approach. First, we fitted calibration regressions, with the CT indices, based on photo counts from single camera traps, as the exposure variable and CMR-based abundance estimates as the ground-truthing variable. In the case of tundra vole, for which several camera traps were used within the same local population, we also assessed to what extent aggregating data over several camera traps improved the fit of the calibration regression, i.e., treating the cameras as spatial replicates. As the camera traps provide continuous-time data, we assessed which temporal resolution (i.e., time-window) of the camera trap data was optimal, in the sense of providing the best goodness-of-fit calibration regression (i.e., maximized the  $R^2$ ). In the second step, we performed inverse prediction to estimate vole abundance using the optimal CT index and evaluated the predictive performance of the model using k-fold cross-validation, bias, and a classification metric for three abundance classes.

## Materials and Methods

### Study areas and species

The data were obtained from two study areas in sub-arctic Norway (Fig. 1) where long-term monitoring of vole populations is ongoing by means of CMR-trapping. Regional-scale population dynamics of gray-sided vole were monitored in Porsanger (N 70.05°, E 24.97°) with multiple trapping stations spaced along a 170 km transect (Nicolau et al., 2020). The sampling was conducted in a mountain birch forest, where the gray-sided vole is the most common species within a community with four

other rodent species (Yoccoz & Ims, 2004). The phases of the 4-year population cycle exhibit a great deal of spatial synchrony across the sampled region (Nicolau et al., [in press](#)). In the case of the tundra vole, local population dynamics were monitored within an area of 1 km<sup>2</sup> on the small oceanic island of Håkøya (N 69.67°, E 18.83°), where the tundra vole is the only rodent species present. The population is distributed on patches of coastal meadows (Soininen et al., 2015), which is the preferred habitat for this species in the Arctic and boreal ecosystem (Soininen et al., 2018; Tast, 1966).

## Sampling design

### CMR-trapping

CMR-trapping was conducted with baited Ugglan No. 2 live traps during the snow-free seasons in the years 2018–2020. Unless previously marked, trapped animals were marked with a passive-induced transponder (PIT)-tag, and the individual covariates *weight* and *sex* were recorded.

For the gray-sided vole monitoring, the trapping was conducted on 15 trapping stations spaced along the study transect (Fig. 1). Each trapping station consisted of a standardized grid with 16 live traps, covering an area of about 0.5 ha (Ehrich et al., 2009). In each of the 3 years, trapping was conducted in three sessions: middle of June, beginning of August, and middle of September. During each session, the trapping was conducted over two consecutive trapping days, following a trap-setting day (see Ehrich et al., 2009 for more details).

For the tundra vole monitoring, trapping was conducted in variably shaped and sized coastal meadow patches. For the purpose of the present study, we defined 4 sampling stations with sizes (approximately 0.5 ha) and trapping grids (10–20 live traps) that were comparable to the sampling stations of the gray-sided vole monitoring. However, in contrast to the widely spaced trapping stations in the regional-scale monitoring of the gray-sided vole, the adjacent tundra vole trapping stations were considered to cover the same local population. CMR-trapping of tundra voles was conducted monthly from June to October (i.e., five trapping sessions) in each of the 3 years. As the trappability of tundra voles is lower than that of gray-sided voles (Øvrejorde, 2007), the tundra vole trapping was conducted over three consecutive days per session. Trappability was further enhanced by pre-baiting the live traps 1 day prior to the first trap night in each session.

### CMR-based abundance estimation

To address the sampling error associated with capture heterogeneity, abundances were estimated using the

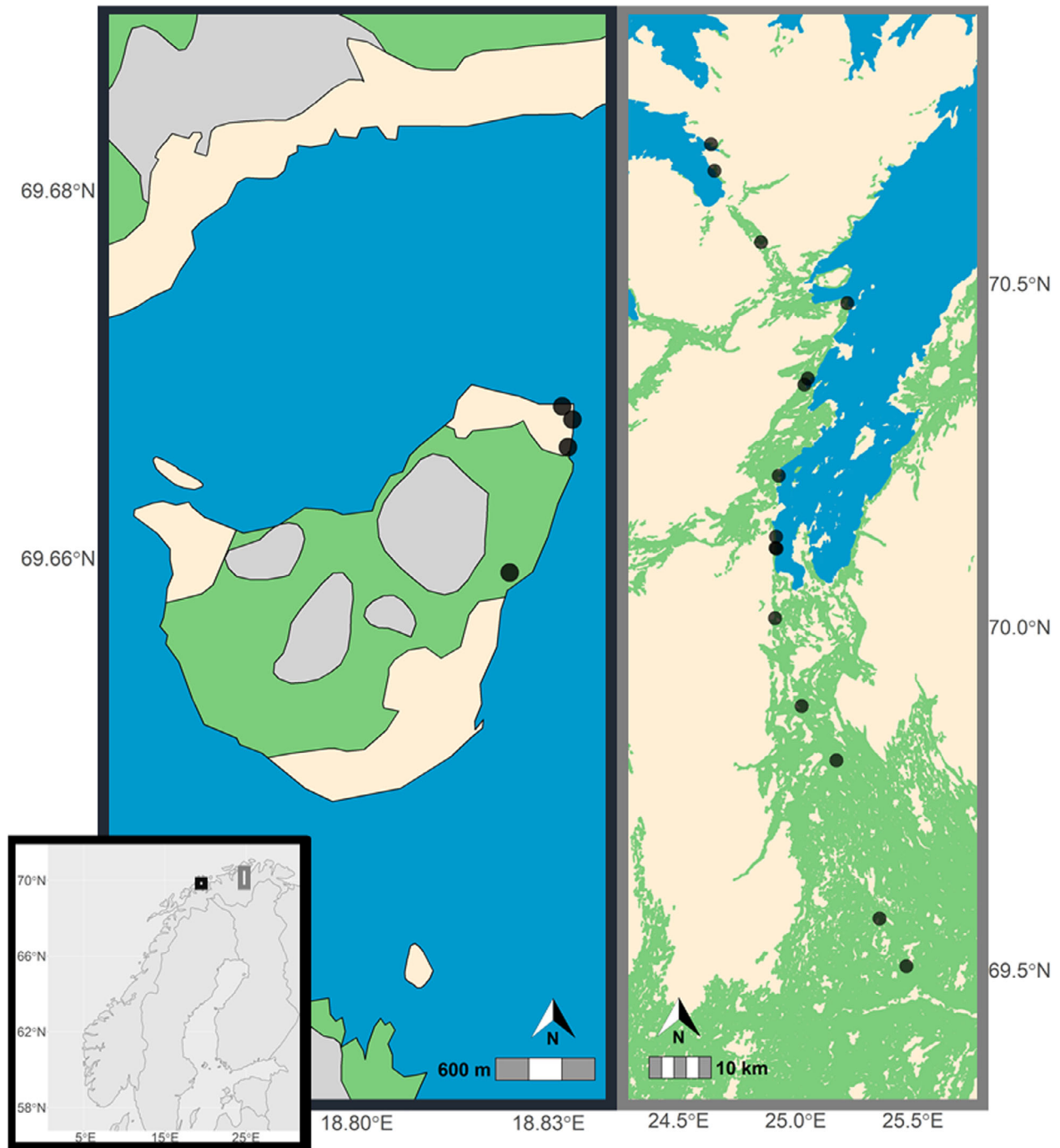


**Figure 1.** Maps of the study areas. Bottom left: regional map of Fennoscandia with the two study areas marked with different colored rectangles (Håkøya in black and Porsanger in gray). Left: Håkøya study area for the tundra vole. Right: Porsanger study area for the gray-sided vole. Black dots denote sampling stations, green hue is forest, light yellow corresponds to non-forested areas on dry ground (e.g., alpine or coastal heaths), gray is mire and blue is sea. Notice the different scales of the two study area maps.

capture histories of each of the trapped individuals. This was based on the CR-INLA method presented by Nicolau et al. (2020), which allows incorporating both observed and unobserved heterogeneity into the estimation of

capture probabilities and abundance. This method makes use of the conditional likelihood framework (reviewed in Huggins & Hwang, 2011) to first estimate the individual capture probabilities (obtained using the efficient

Bayesian approach INLA, Simpson et al., 2017) and then using those probabilities to estimate abundance with the widely used Horvitz-Thompson estimator (Horvitz & Thompson, 1952). Specifically for this study, individual capture probabilities were assumed to have a temporal effect (model  $M_{th}$  in Otis et al., 1978). We then fitted a multinomial regression model, where the logit-transformed probabilities of the capture histories were modeled in terms of the individual variables *weight* and *sex* (observed heterogeneity) and independent random effects for the trapping station, to account for unobserved spatially-varying capture heterogeneity. Subsequently, the resulting abundance estimates were standardized according to the number of live traps at each trapping location.

### Camera trapping and abundance indices

In November 2017 (tundra vole) and June 2018 (gray-sided vole), a single camera trap was placed within each of the CMR grids, for a total of 15 camera traps in Porsanger and 4 in Håkkøya. We used the tunnel trap developed by Soininen et al. (2015). The tunnel trap consists of a metal tunnel with a movement-triggered camera attached to the roof. The device is placed in natural small mammal runways, identified by clues in the field. For further descriptions of camera trap setup and settings see Appendix A.2 and Mölle et al. (2021).

As the camera trap continuously records images throughout the year, we must first obtain discretized CT indices to be calibrated. For this, we obtain different CT indices based on the number of species-specific photo counts during different time windows (Fig. 2). Let  $X_k$ ,  $k = -11, \dots, 11$ , denote the number of photos counted

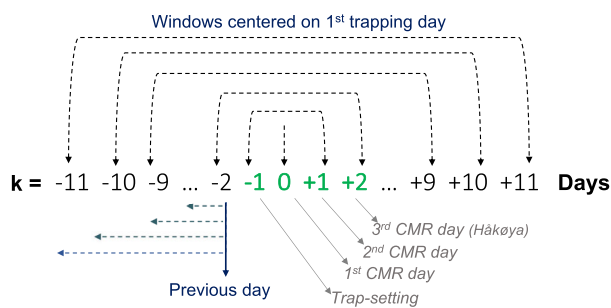


**Figure 2.** Schematic representation of the time windows used to aggregate photo counts for the camera trap-based abundance indices. Days related to the CMR-trapping are presented in green, with day 0 corresponding to the first capture day (following trap-setting on the previous day; day -1), followed by one (gray-sided vole) or two (tundra vole) capture days. Two types/groups of time windows are defined: CMR-encompassing, centered on the first CMR day and thus including all days with activated live traps, shown by the upper set of vertical arrows; and CMR-preceding, for the days preceding the trap-setting day, shown by the set of the bottom left vertical arrows.

on day  $k$  relative to the first day of CMR-trapping ( $k = 0$ ). The different temporal windows  $I$  denote intervals of  $d$  days. Each CT index is then defined as the average CT counts per day for a given  $I$ , given by  $Y_I = \frac{1}{d} \sum_{k \in I} X_k$ .

We define two types/groups of time windows, depending on whether the window encompassed the CMR trapping or preceded it. We make this distinction to account for the potential confounding effect of the entrapment of animals during CMR trapping (i.e., considering that animals in live traps cannot be camera trapped). For the CMR-preceding intervals, we assessed the windows  $I = [k, -2]$ , where  $k = -11, \dots, -2$ . For the CMR-encompassing intervals, we used the windows  $I = [-k, k]$ , where  $k = 0, \dots, 11$ .

### Calibration analysis

To understand if the CT indices reflect abundance, we perform calibration analysis using the CT indices for each time window as the exposure variable, and the CMR-based abundance estimates as the ground-truthing variable. This analysis consists of two steps: first, calibrating CMR abundance as a function of the CT index (with associated error); and second, performing inverse prediction to obtain the estimate of abundance and associated uncertainty based on the CT index. The second step is then further used to perform model validation.

For gray-sided voles, the calibration data includes a total of 115 calibration points (15 trapping sites for 8 trapping sessions, with one camera trap missing observations in 5 trapping sessions due to technical issues), while there are 60 calibration points (4 trapping sites for 15 trapping sessions) for the tundra voles (see Appendix A.1). As the 4 trapping stations for the tundra vole are in close proximity and can be considered to regard the same local population, we additionally perform a calibration analysis with the abundance indices and estimates averaged across all stations, which yields 15 calibration points.

### Calibration regression

As the first step, we establish a calibration regression between the variables of interest. Let  $Y_{I,s,t}$  denote the CT index for a given temporal window  $I$ , measured at station  $s$  and trap season  $t$ . A linear relationship between the CT index and the CMR abundance ( $N_{s,t}$ ) is best fitted on a log scale. A linear regression model is thus formulated by

$$\log(Y_{I,s,t} + 1) = \beta_0 + \beta_1 \log(N_{s,t} + 1) + \epsilon_{I,s,t}, \quad (1)$$

where  $\log(Y_{I,s,t} + 1)$  corresponds to the log CT index for the given time window  $I$ , location  $s$ , and trapping season

$t$ .  $\beta_0$  and  $\beta_1$  are coefficients to be estimated to define the calibration line for each  $I$ . The set  $\{\epsilon_{I,s,t}\}$  denotes error terms that are assumed to be independent and normally distributed with homogeneous variance. The number 1 is added to ensure positive arguments of the log function. The ordinary coefficient of determination  $R^2$  is used as a measure of the goodness-of-fit.

### Inverse prediction and model validation

After having established a calibration regression between the ground-truthing variable and the exposure variable, we can now perform inverse prediction which provides the appropriate uncertainty interval for the exposure variable. For this, we use the R-package *investr* (Greenwell & Schubert Kabban, 2014) to compute the Wald 95% prediction interval for a new observation,  $\hat{x}_0 = \frac{\hat{y}_0 + \beta_0}{\beta_1}$ , where  $\hat{x}_0$  is the CMR-abundance estimate using the observed CT-index  $\hat{y}_0$ , and  $\beta_0$  and  $\beta_1$  denote estimates of the coefficients of the calibration regression.

To assess the predictive performance of the calibration model with the time window with the highest  $R^2$  value, we employ a k-fold cross-validation approach. Specifically, we remove all calibration points for a given station and estimate the coefficients of (1) using the remaining stations. We then predict the CMR abundances given the corresponding CT index of the excluded station. This is repeated for all stations, thus being equivalent to a 15-fold cross-validation approach for the gray-sided vole and a 4-fold cross-validation approach for tundra voles. For the spatially aggregated tundra vole calibration, performing cross-validation is not feasible (only 15 calibration points at a single spatial location).

Different measures of predictive performance are computed. These include coverage of the 95% prediction interval for the explanatory variables log CMR-abundances, the mean absolute error, and the root mean squared error. Additionally, we define an ecological classification metric (ECM) which intends to provide qualitative information on predictions that are functionally relevant for cyclic populations (i.e., cycle phases). We define the following three population density categories: low-abundances (low phase of the cycle), intermediate abundances, and high abundances (high phase). The high and low abundances are defined as the 25% and 75% quantiles of the respective sample distributions for each species. The ECM is thus defined as the proportion of times the true observed log-abundance value and the predicted value belong to the same category. The analysis was conducted in R 4.0.3 (R Core Team, 2020).

## Results

### Abundance estimates and indices

Annual means of the CMR-based abundance estimates reveal the phases/years of population increase (2018), peak (2019), and crash (2020) for both vole species (Fig. 3). The distributions of the standardized abundance estimates and indices were similar between the species (Table 1). Moreover, neither the overall means nor the variance in the CT indices differed notably between species or time windows (Table 1 and Fig. 4). However, there was a difference in the temporal autocorrelations of daily CT counts between the two species. While the estimated auto-correlations decreased linearly over time with relatively little scatter for the gray-sided vole, the estimated auto-correlations for the tundra vole showed a steeper decrease over the first 4 days before it leveled off with a large scatter. Furthermore, for the gray-sided vole, there were some indications of a small increase in the mean number of photos taken per day during the days when the live trapping was conducted, which might suggest a possible interaction between the two methodologies.

### Linear calibration regression

The linear calibration regressions based on the single camera trap per trapping station yielded  $R^2$ -values that greatly differed between the two species. The  $R^2$ -values for all time windows are substantially higher for the gray-sided vole than the tundra vole (Fig. 5). For the gray-sided vole, all time windows for the CMR-encompassing group yielded similarly good fits (all  $R^2 > 0.5$  except for  $Y_{[0,0]}$ ). The best fitting calibration model ( $R^2 = 0.58$ , coefficients:  $\beta_0 = 0.15$ ;  $\beta_1 = 1.44$ ) was obtained for the 5-day time window that encompassed the live-trapping session ( $Y_{[-2,2]}$ ). This regression model fulfilled the assumptions regarding log-scale linearity. For the tundra vole, the best fit ( $R^2 = 0.21$ , coefficients:  $\beta_0 = 0.37$ ;  $\beta_1 = 1.28$ ) was obtained for the CT-index based on a single day before the onset of the live trapping ( $Y_{[-2,-2]}$ ). For the other time windows (all  $R^2 < 0.2$ ) the difference between the two groups of time windows was small. When the data were aggregated over four adjacent sampling stations for the tundra vole population, the fit of the calibration function improved substantially ( $R^2 = 0.81$ , Coefficients:  $\beta_0 = -0.16$ ;  $\beta_1 = 2.17$ , Fig. 6).

### Inverse prediction and validation

As could be expected from the differences in the goodness-of-fit of the calibration regression (i.e. the  $R^2$

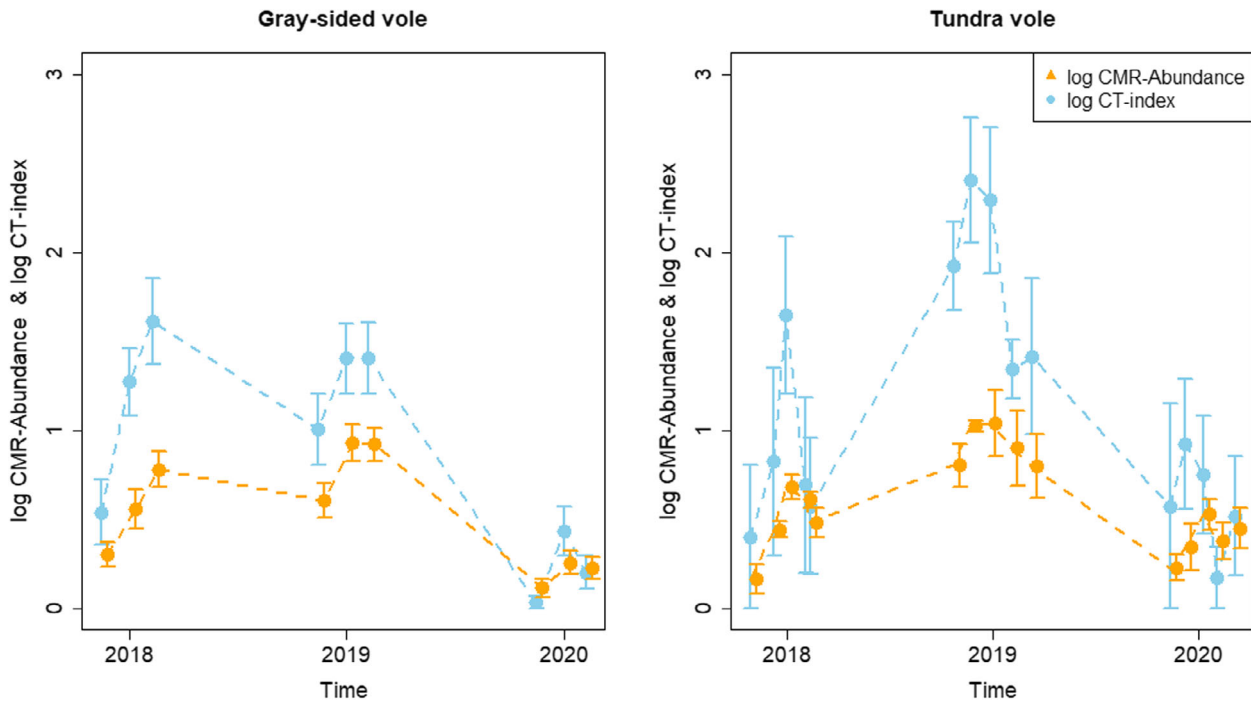


**Figure 3.** Population dynamics over trapping seasons (within years) and years based on log-scale CT-abundance indices (blue circles) and log CMR-abundance estimates standardized by the number of traps (orange circles). The indices and estimates represent means with standard error bars over all trapping stations for the two species. The optimal time windows for the CT index are used for both species (see Fig. 5). 2018 corresponds to the increase phase, 2019 the peak phase, and 2020 the crash phase of the rodent cycle.

**Table 1.** Distribution statistics (arithmetic mean, standard deviation, and range) for the standardized log-transformed abundances estimates (CMR-based;  $\log(\text{abundance}/N \text{ traps})$ ) and log CT-indices ( $\log(\text{CT-counts}/N \text{ days})$ ) for each trapping station as they are used in the calibration regression models. The CT indices are given for the time window that provided the best-fitting calibration regression (see Fig. 5).

Metric	Statistic	Gray-sided vole	Tundra vole
CMR-estimates	Mean	0.54	0.59
	STDev	0.44	0.34
	Range	0–1.63	0–1.59
CT-indices	Mean	0.93	1.13
	STDev	0.84	0.94
	Range	0–3.10	0–3.22

values), the prediction intervals derived by the inverse regression were wider for the tundra vole than for the gray-sided vole (Fig. 7). The RMSE value (indicating the width of the interval) was almost twice as high for the tundra vole compared to the gray-sided vole, and the bias was about three times higher (Table 2). In terms of classifying abundances based on the single camera traps with respect to the three abundance classes (*cf.* ECM metrics in Table 2), close to two-thirds of the instances were

correctly classified for the gray-sided vole, compared to roughly one-third for the tundra vole.

## Discussion

We have here assessed the adequacy of using photo counts, from the tunnel-based camera trap developed by Soininen et al. (2015), as abundance metrics to study population dynamics of two ecologically important vole species that exhibit multi-annual cycles in boreal and Arctic ecosystems. Our assessment employed a calibration approach, in which different temporally scaled CT indices were calibrated against CMR-based abundance estimates. In order to be adequate, abundance indices are required to have proportional (e.g., linear) relationships to the true abundance as well as reasonable precision. While the true abundance is not known, like in most real-world examples, we assume that the CMR-based abundance estimates approximate true abundance relatively well. Considering that count-based camera trap indices (i.e. the number of motion-triggered animal passages) also reflect animal behavior (e.g. spacing behavior; *sensu* Krebs, 1996), which for long has been known to be density and phase-dependent in cyclic vole populations (Chitty, 1960; Krebs, 2013), the assumption regarding proportionality can be violated.

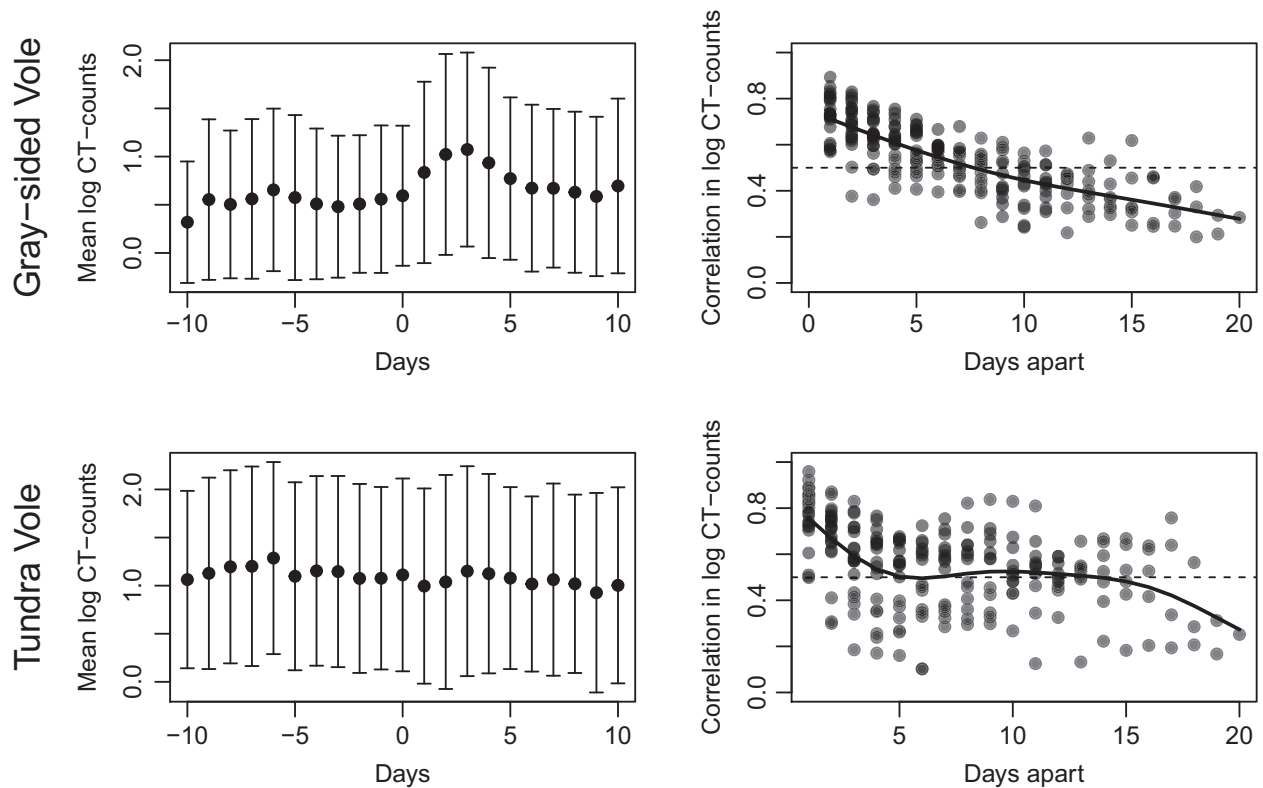


**Figure 4.** CT-count variation and temporal correlations. Left panels: mean of all the log CT counts on each day relative to the trapping experiment (according to Fig. 2), with standard deviation bars. Right panels: temporal auto-correlations in daily log CT counts per trap and trapping session as a function of temporal distance, i.e., days apart. The solid lines are non-parametric smooth regression lines from the `smooth.spline` function of the `stats` R-package (version 4.0.3).

While the relationship between the CT index and CMR abundance seems to be proportional (on the log scale) for both vole species, the precision of the abundance indices based on single camera traps differed considerably between them. For the gray-sided vole, the CT indices from the single camera traps correlated well with the CMR abundance estimates from the matched live-trapping grids, whereas the equivalent correlation for the tundra vole was poorer. Accordingly, validation metrics of the inverse regressions showed that the abundance predictions based on single camera traps were substantially better for the gray-sided vole than the tundra vole. Compared with two previous calibration studies of non-cyclic vole populations in boreal America, the goodness of fit of the calibration regression for the cyclic gray-sided vole population ( $R^2 = 0.58$ ) performed equally well (Villette et al., 2015 obtained  $R^2 = 0.59$  for northern red-backed vole *Myodes rutilus*) or better (Parsons et al., 2021 obtained  $R^2 = 0.34$  for voles *Microtus* sp. and *Myodes gapperi*). The two American studies employed a different camera trap; i.e. open cameras mounted in front of the entrance of baited live traps. Moreover, these previous

studies used aggregated CT indices over 15–16 (Villette et al., 2015) and 16–20 camera traps (Parsons et al., 2021) per live-trapping grid, which was twice the size of our grids. The fact that we obtained at least an equally good calibration for the gray-sided vole with a single camera trap, and an even better calibration ( $R^2 = 0.81$ ) for the tundra vole when aggregating the data over only 4 camera traps, indicates that our unbaited permanently deployed tunnel-based traps are more efficient in capturing vole dynamics compared to the free-standing and moveable camera traps in Villette et al. (2015) and Parsons et al. (2021).

The differences in goodness-of-fit of the calibrations (and thus also the precision of the abundance predictions) of gray-sided voles and tundra voles are reflected by the different optimal time windows and the temporal auto-correlations of CT counts for the two species. The optimized time window for the gray-sided vole was longer (5 days including the live trapping days) and less temporally distinct (high  $R^2$ -values for a wide range of time windows) than for the tundra voles. The best time window for the tundra vole was based on a single day just



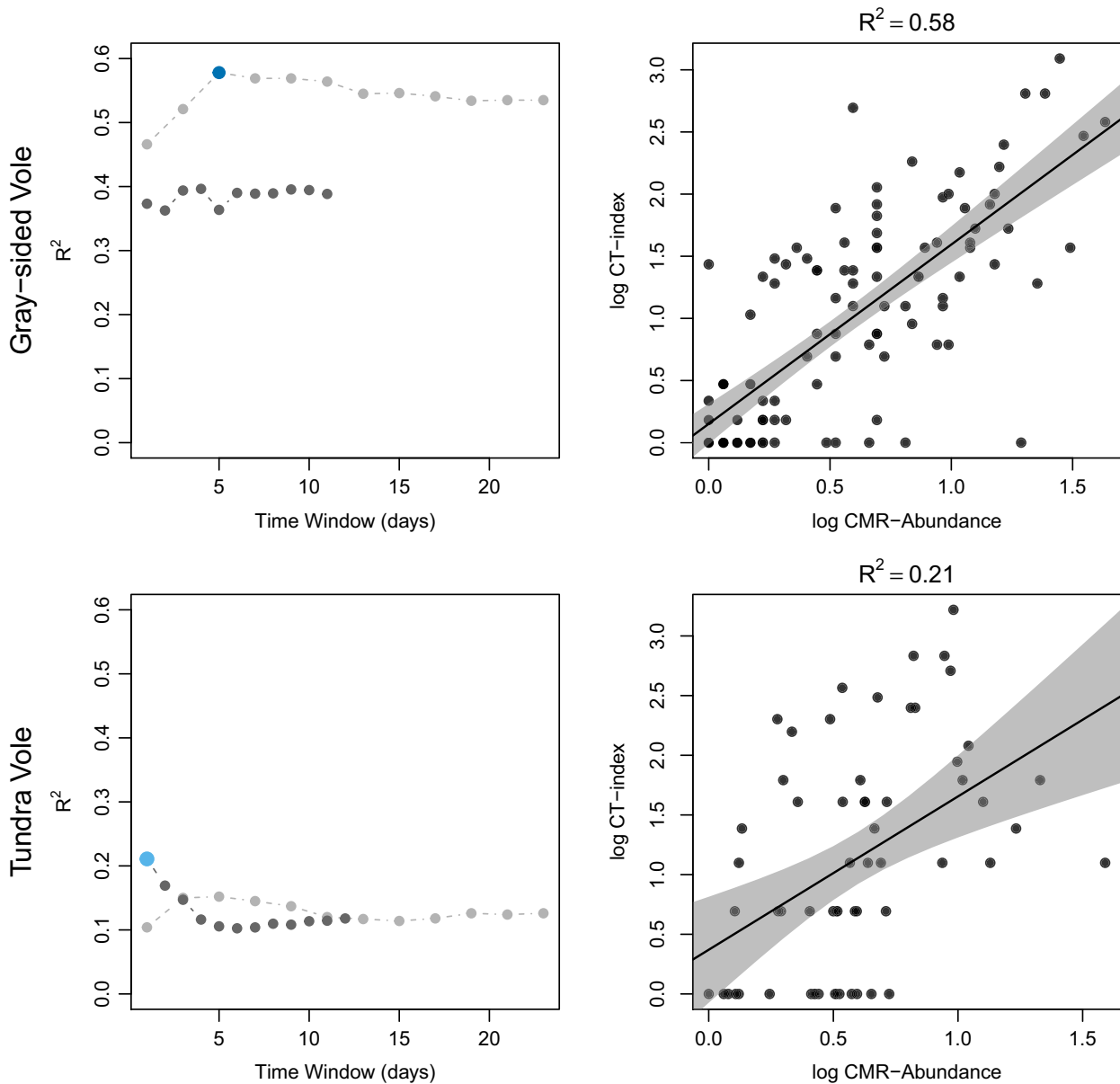


**Figure 5.** Statistics for linear calibration regressions. Left panels:  $R^2$  values for the calibration linear regressions fitted to the two groups of time windows (CRM-encompassing: light gray symbols and CMR-preceding: dark gray symbols). The highest  $R^2$  values for each species are marked with an enlarged blue dot. Right panels: Data points and regression lines with 95% confidence intervals for the species-specific linear calibration models that yielded the highest  $R^2$ .

prior to the onset of the live-trapping sessions. Accordingly, the auto-correlations of the daily camera counts dropped faster and had a generally higher scatter for the tundra vole than the gray-sided vole. We believe this can be explained by the fact that the two vole species differ with respect to how their populations are spatio-socially organized (Bondrup-Nielsen & Ims, 1990; Ims, 1987b). Due to female territoriality, gray-sided voles are more

evenly spaced within their habitat than tundra voles where females form spatially clustered kin groups. These local tundra vole kin groups are temporally unstable since females frequently shift home ranges (Tast, 1966). Consequently, local-scale abundance dynamics of tundra voles are typically characterized by a high turnover (Andreassen & Ims, 2001) and weak auto-correlations (Ims & Andreassen, 1999). This is important as we have only 1

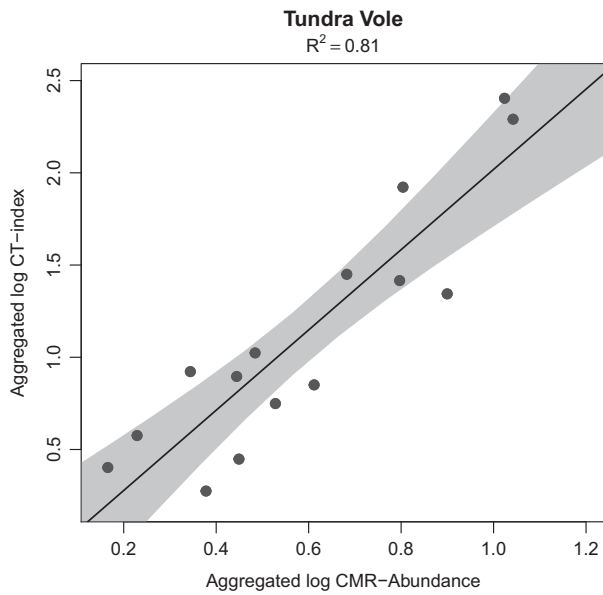


**Figure 6.** Calibration regression for tundra vole using aggregated data across all stations for the best fitting time window ( $Y_{[-2,-2]}$ ). Coefficients:  $\beta_0 = -0.16$ ;  $\beta_1 = 2.17$ ;  $P$ -value  $< 0.001$ .

camera trap within a 0.5 ha live trapping grid compared to 16 live traps spanning the whole range of the grid. Hence, a tundra vole including the camera trap in its home range might shift home range to still include a

**Table 2.** Prediction metrics for the models with highest  $R^2$  for both the gray-sided Vole ( $Y_{[-2,2]}$ ) and the tundra vole ( $Y_{[-2,-2]}$ ).

Species	Coverage	ECM <sub>A</sub>	Bias	RMSE
Gray-sided vole	0.957	0.609	-0.004	0.385
Tundra vole	0.933	0.350	0.013	0.701

subset of the trapping grid (and therefore also some of the live traps), but not the camera trap. The much-improved fit of the tundra vole calibration regression, when based on 4 instead of 1 camera trap, is most likely due to the effect of smoothing out the large small-scale spatio-temporal variability. This result underlines the benefit of spatially replicating camera traps within the same location/local population, which has also been highlighted by other authors (Kolowski et al., 2021). However, our study also shows that only a few tunnel-based camera traps may be needed to get adequate abundance indices for both vole species. In fact, a single camera trap was able to capture the main features of the cyclic dynamics of gray-sided vole. This indicates there may be a potential for conducting spatially extensive monitoring, for instance in order to estimate patterns of large-scale spatial population synchrony (Bjørnstad et al., 1999), even with a limited number of camera traps available. In general, the purpose of the monitoring should be guiding spatial

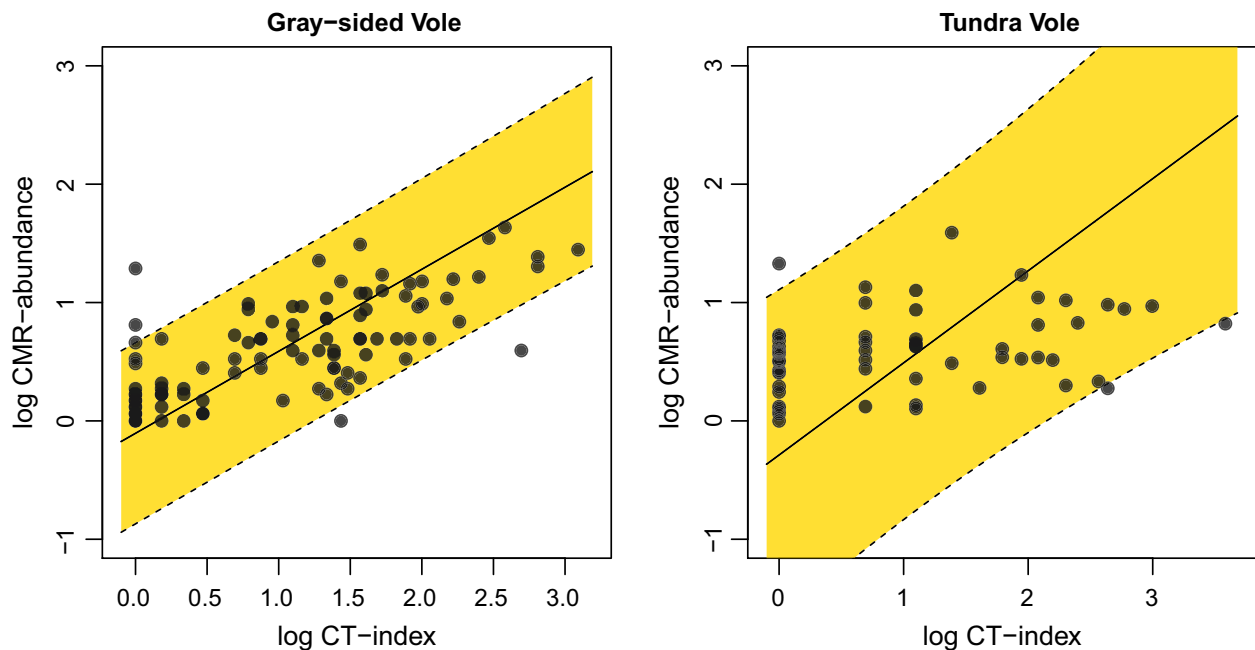


**Figure 7.** Inverse prediction plots for the CT-index windows yielding the best goodness-of-fit for each region, on the log scale. The Wald 95% confidence intervals are colored in yellow, and the data points are plotted in black dots.

monitoring designs (Lindenmayer & Likens, 2009), both in terms of grain and extent of the sampling (Wiens, 1989). With regard to rodent population dynamics, much interest is still devoted to elucidating the drivers of cyclicity (Oli, 2019). For instance, elucidating the role of predation opts for a design that encompasses the relatively small scale of both prey (rodents) and larger scale of predator (e.g. mustelids). This may be achieved by a two-level, spatial hierarchical design with replication at both the scale of the prey and the predator (Kleiven et al., 2021). Moreover, much current key interest is devoted to the influence of climate on rodent population dynamics, which may opt for spatial design encompassing climate gradients (Ims et al., 2011). Spatially extensive sampling by means of camera traps is facilitated by low fieldwork effort. Each camera trap needs to be only visited once per year (Möller et al., 2021), which makes also including remote areas in the sampling feasible.

We believe that the greatest asset of the tunnel-based camera trap employed in our study is its ability to yield population metrics year-round, with a finer temporal resolution than any other presently available method. For small rodents with multi-annual cycles, the transitions between the different cyclic phases (e.g., between peak and crash) can be very rapid and take place at any time of the year (Krebs, 2013). By providing reliable abundance indices for time windows as short as a few days, camera traps radically enhance our options for identifying the drivers of cyclic rodent dynamics. Strongly density-dependent interactions and rapid community-level dynamics have long been assumed to be driving rodent cycles (Barraquand et al., 2017; Hansson & Henttonen, 1988; Turchin & Hanski, 2001). Assumed key interactions—such as those between voles and small mustelids—have been beyond the reach of thorough investigations owing to the difficulty of obtaining adequately scaled data for both interactants simultaneously (King & Powell, 2007). Our tunnel-based camera traps recorded substantial data (i.e. relatively high number of photo counts) for all members of the small mammal community in both study areas, including small mustelids (least weasel *Mustela nivalis* and stoat *Mustela erminea*), Norwegian lemmings (*Lemmus lemmus*), and shrews (*Sorex* spp.) (see also Möller et al., 2021) and Appendix B.3). While species-interactions based on camera trap data can be analyzed based on absence-presence records within an occupancy modeling framework (Fidino et al., 2019; Rota et al., 2016), abundance metrics are more informative as they allow analyses of the density-dependent interactions that appear to drive population cycles (Stenseth, 1999).

Within arvicoline rodents, the gray-sided vole and the tundra vole represent stark contrasts in terms of spacing and social systems (Bondrup-Nielsen & Ims, 1990) and

thus likely also contrasting in turnover rates of local-scale population dynamics. Hence, we expect camera trap-based abundance indices to be reliable also for other vole species. In general, we propose that four camera traps dispersed over adjacent habitat patches (i.e., akin to our tundra vole case study) will provide adequate data to accurately monitor the local abundance dynamics of cyclic vole populations. Furthermore, we recommend that new studies focus on validating camera trap-based abundance indices for species such as mustelids and lemmings. As true ground-truthing variables for such species (especially mustelids (King & Powell, 2007)) are extremely difficult to obtain, it may be possible to resort to statistical frameworks for unmarked populations to obtain detectability corrected abundance indices (see e.g. Gilbert et al., 2021; Palencia et al., 2021). Such frameworks may also be used to derive unbiased abundance indices from camera trap data during the boreal and Arctic winter when deep snow and harsh climatic conditions hinder formal calibration studies as we have here performed. Hence, although our study highlights the potential of tunnel-based camera traps to likely advance studies of cyclic rodent populations, it also illustrates the need for performing species- and context-specific validation studies.

## Acknowledgments

We thank Hanna Böhner for the invaluable help with the automatic classification of the camera trap images. This work is a contribution from COAT (Climate-ecological Observatory for Arctic Tundra) supported by the RCN (project nr. 245638), COAT Tools supported by UiT, and COAT Tools+ supported by Tromsø Research Foundation. We declare no conflict of interest, that all authors on the manuscript have seen and approved the submitted version, that all authors have substantially contributed to the work, and that all persons entitled to co-authorship have been included.

## References

- Andreassen, H.P. & Ims, R.A. (2001) Dispersal in patchy vole populations: role of patch configuration, density dependence, and demography. *Ecology*, **82**(10), 2911–2926. [https://doi.org/10.1890/0012-9658\(2001\)082\[2911:DIPVPR\]2.0.CO;2](https://doi.org/10.1890/0012-9658(2001)082[2911:DIPVPR]2.0.CO;2)
- Andreassen, H.P., Sundell, J., Ecke, F., Halle, S., Haapakoski, M., Henttonen, H. et al. (2021) Population cycles and outbreaks of small rodents: ten essential questions we still need to solve. *Oecologia*, **195**(3), 601–622. <https://doi.org/10.1007/s00442-020-04810-w>
- Bailey, L.L., MacKenzie, D.I. & Nichols, J.D. (2014) Advances and applications of occupancy models. *Methods in Ecology*

- and Evolution*, 5(12), 1269–1279. <https://doi.org/10.1111/2041-210X.12100>
- Barraquand, F., Louca, S., Abbott, K.C., Cobbold, C.A., Cordoleani, F., DeAngelis, D.L. et al. (2017) Moving forward in circles: challenges and opportunities in modelling population cycles. *Ecology Letters*, 20(8), 1074–1092. <https://doi.org/10.1111/ele.12789>
- Bjørnstad, O.N., Ims, R.A. & Lambin, X. (1999) Spatial population dynamics: analyzing patterns and processes of population synchrony. *Trends in Ecology and Evolution*, 14(11), 427–432. [https://doi.org/10.1016/s0169-5347\(99\)01677-8](https://doi.org/10.1016/s0169-5347(99)01677-8)
- Bondrup-Nielsen, S. & Ims, R.A. (1990) Reversed sexual size dimorphism in microtines: are females larger than males or are males smaller than females? *Evolutionary Ecology*, 4(3), 261–272. <https://doi.org/10.1007/bf02214334>
- Boonstra, R., Andreassen, H.P., Boutin, S., Hušek, J., Ims, R.A., Krebs, C.J. et al. (2016) Why do the boreal forest ecosystems of northwestern Europe differ from those of western North America? *Bioscience*, 66(9), 722–734. <https://doi.org/10.1093/biosci/biw080>
- Boonstra, R. & Krebs, C.J. (1978) Pitfall trapping of *Microtus townsendii*. *Journal of Mammalogy*, 59(1), 136–148. <https://doi.org/10.2307/1379883>
- Burton, A.C., Neilson, E., Moreira, D., Ladle, A., Steenweg, R., Fisher, J.T. et al. (2015) Review: wildlife camera trapping: a review and recommendations for linking surveys to ecological processes. *Journal of Applied Ecology*, 52(3), 675–685. <https://doi.org/10.1111/1365-2664.12432>
- Capizzi, D., Bertolino, S. & Mortelliti, A. (2014) Rating the rat: global patterns and research priorities in impacts and management of rodent pests. *Mammal Review*, 44(2), 148–162. <https://doi.org/10.1111/mam.12019>
- Chitty, D. (1960) Population processes in the vole and their relevance to general theory. *Canadian Journal of Zoology*, 38(1), 99–113. <https://doi.org/10.1139/z60-011>
- Cornulier, T., Yoccoz, N.G., Bretagnolle, V., Brommer, J.E., Butet, A., Ecke, F. et al. (2013) Europe-wide dampening of population cycles in keystone herbivores. *Science*, 340(6128), 63–66. <https://doi.org/10.1126/science.1228992>
- Diefenbach, D.R., Conroy, M.J., Warren, R.J., James, W.E., Baker, L.A. & Hon, T. (1994) A test of the scent-station survey technique for bobcats. *The Journal of Wildlife Management*, 58(1), 10. <https://doi.org/10.2307/3809543>
- Ehrich, D., Schmidt, N.M., Gauthier, G., Alisauskas, R., Angerbjörn, A., Clark, K. et al. (2019) Documenting lemming population change in the Arctic: can we detect trends? *Ambio*, 49(3), 786–800. <https://doi.org/10.1007/s13280-019-01198-7>
- Ehrich, D., Yoccoz, N.G. & Ims, R.A. (2009) Multi-annual density fluctuations and habitat size enhance genetic variability in two northern voles. *Oikos*, 118(10), 1441–1452. <https://doi.org/10.1111/j.1600-0706.2009.17532.x>
- Eisenhart, C. (1939) The interpretation of certain regression methods and their use in biological and industrial research. *The Annals of Mathematical Statistics*, 10(2), 162–186. <https://doi.org/10.1214/aoms/1177732214>
- Fidino, M., Simonis, J.L. & Magle, S.B. (2019) A multistate dynamic occupancy model to estimate local colonization–extinction rates and patterns of co-occurrence between two or more interacting species. *Methods in Ecology and Evolution*, 10(2), 233–244. <https://doi.org/10.1111/2041-210X.13117>
- Gilbert, N.A., Clare, J.D.J., Stenglein, J.L. & Zuckerberg, B. (2021) Abundance estimation of unmarked animals based on camera-trap data. *Conservation Biology: The Journal of the Society for Conservation Biology*, 35(1), 88–100. <https://doi.org/10.1111/cobi.13517>
- Gopalswamy, A.M., Mohan Delampady, K., Ullas Karanth, N., Kumar, S. & Macdonald, D.W. (2015) An examination of index-calibration experiments: counting tigers at macroecological scales. *Methods in Ecology and Evolution*, 6(9), 1055–1066. <https://doi.org/10.1111/2041-210x.12351>
- Greenwell, B.M. & Schubert Kabban, C.M. (2014) Investr: an R package for inverse estimation. *The R Journal*, 6(1), 90. <https://doi.org/10.32614/rj-2014-009>
- Hansen, T.F., Stenseth, N.C. & Henttonen, H. (1999) Multiannual vole cycles and population regulation during long winters: an analysis of seasonal density dependence. *The American Naturalist*, 154(2), 129–139. <https://doi.org/10.1086/303229>
- Hanski, I., Henttonen, H. & Hansson, L. (1994) Temporal variability and geographical patterns in the population density of microtine rodents: a reply to xia and boonstra. *The American Naturalist*, 144(2), 329–342. <https://doi.org/10.1086/285678>
- Hansson, L. & Henttonen, H. (1988) Rodent dynamics as community processes. *Trends in Ecology and Evolution*, 3(8), 195–200. [https://doi.org/10.1016/0169-5347\(88\)90006-7](https://doi.org/10.1016/0169-5347(88)90006-7)
- Henden, J.-A., Ehrich, D., Soininen, E.M. & Ims, R.A. (2021) Accounting for food web dynamics when assessing the impact of mesopredator control on declining prey populations. *Journal of Applied Ecology*, 58(1), 104–113. <https://doi.org/10.1111/1365-2664.13793>
- Hörnfeldt, B., Hipkiss, T. & Eklund, U. (2005) Fading out of vole and predator cycles? *Proceedings of the Royal Society B: Biological Sciences*, 272(1576), 2045–2049. <https://doi.org/10.1098/rspb.2005.3141>
- Horvitz, D.G. & Thompson, D.J. (1952) A generalization of sampling without replacement from a finite universe. *Journal of the American Statistical Association*, 47(260), 663–685. <https://doi.org/10.1080/01621459.1952.10483446>
- Huggins, R. & Hwang, W.-H. (2011) A review of the use of conditional likelihood in capture-recapture experiments. *International Statistical Review*, 79(3), 385–400. <https://doi.org/10.1111/j.1751-5823.2011.00157.x>
- Ims, R.A. & Andreassen, H.P. (1999) Spatial demographic synchrony in fragmented populations. In: Barrett, G. & Peles, J. (Eds.) *The ecology of small mammals at the*

- landscape level: experimental approaches. New York, NY: Springer-Verlag, pp. 129–145. [https://doi.org/10.1007/978-0-387-21622-5\\_7](https://doi.org/10.1007/978-0-387-21622-5_7)
- Ims, R.A. & Fuglei, E. (2005) Trophic interaction cycles in tundra ecosystems and the impact of climate change. *Bioscience*, **55**(4), 311–322. [https://doi.org/10.1641/0006-3568\(2005\)055\[0311:TICITE\]2.0.CO;2](https://doi.org/10.1641/0006-3568(2005)055[0311:TICITE]2.0.CO;2)
- Ims, R.A., Killengreen, S.T., Ehrich, D., Flagstad, Ø., Hamel, S., Henden, J.-A. et al. (2017) Ecosystem drivers of an arctic fox population at the western fringe of the eurasian arctic. *Polar Research*, **36**(sup1), 8. <https://doi.org/10.1080/17518369.2017.1323621>
- Ims, R.A., Yoccoz, N.G. & Killengreen, S.T. (2011) Determinants of lemming outbreaks. *Proceedings of the National Academy of Sciences*, **108**(5), 1970–1974. <https://doi.org/10.1073/pnas.1012714108>
- Ims, R.A. (1987a) Male spacing systems in microtine rodents. *The American Naturalist*, **130**(4), 475–484. <https://doi.org/10.1086/284725>
- Ims, R.A. (1987b) Responses in spatial organization and behaviour to manipulations of the food resource in the vole *Clethrionomys rufocanus*. *The Journal of Animal Ecology*, **56**(2), 585. <https://doi.org/10.2307/5070>
- Jennelle, C.S., Runge, M.C. & MacKenzie, D.I. (2002) The use of photographic rates to estimate densities of tigers and other cryptic mammals: a comment on misleading conclusions. *Animal Conservation*, **5**(2), 119–120. <https://doi.org/10.1017/S1367943002002160>
- Jensen, P.M., Stenseth, N.C. & Framstad, E. (1993) Trappability of the norwegian lemming (*Lemmus lemmus*). In: Stenseth, N.C. & Ims, R.A. (Eds.) *The biology of lemmings*. London: Academic Press, pp. 547–554.
- King, C.M. & Powell, R.A. (2007) *The natural history of weasels and stoats: ecology, behavior, and management*. New York, NY: Oxford University Press.
- Kleiven, E.F., Barraquand, F., Gimenez, O., Henden, J.-A., Ims, R.A., Soininen, E.M. et al. (2021) A dynamic occupancy model for interacting species with two spatial scales. *bioRxiv*. <https://doi.org/10.1101/2020.12.16.423067>, <https://www.biorxiv.org/content/early/2021/03/05/2020.12.16.423067>
- Kleiven, E.F., Henden, J.-A., Ims, R.A. & Yoccoz, N.G. (2018) Seasonal difference in temporal transferability of an ecological model: near-term predictions of lemming outbreak abundances. *Scientific Reports*, **8**(1), 15252. <https://doi.org/10.1038/s41598-018-33443-6>
- Kolowski, J.M., Oley, J. & McShea, W.J. (2021) High-density camera trap grid reveals lack of consistency in detection and capture rates across space and time. *Ecosphere*, **12**(2), e03350. <https://doi.org/10.1002/ecs2.3350>
- Korpela, K., Delgado, M., Henttonen, H., Korpimäki, E., Koskela, E., Ovaskainen, O. et al. (2013) Nonlinear effects of climate on boreal rodent dynamics: mild winters do not negate high-amplitude cycles. *Global Change Biology*, **19**(3), 697–710. <https://doi.org/10.1111/gcb.12099>
- Krebs, C.J. (1996) Population cycles revisited. *Journal of Mammalogy*, **77**(1), 8–24. <https://doi.org/10.2307/1382705>
- Krebs, C.J. (2013) *Population fluctuations in rodents*. Chicago, IL: University of Chicago Press.
- Krebs, C.J., Boonstra, R., Gilbert, S., Reid, D., Kenney, A.J. & Hofer, E.J. (2011) Density estimation for small mammals from livetrapping grids: rodents in northern Canada. *Journal of Mammalogy*, **92**(5), 974–981. <https://doi.org/10.1644/10-MAMM-A-313.1>
- Lambin, X., Petty, S.J. & Mackinnon, J.L. (2000) Cyclic dynamics in field vole populations and generalist predation. *Journal of Animal Ecology*, **69**(1), 106–119. <https://doi.org/10.1046/j.1365-2656.2000.00380.x>
- Legagneux, P., Gauthier, G., Lecomte, N., Schmidt, N.M., Reid, D., Cadieux, M.C. et al. (2014) Arctic ecosystem structure and functioning shaped by climate and herbivore body size. *Nature Climate Change*, **4**(5), 379–383. <https://doi.org/10.1038/nclimate2168>
- Lindenmayer, D.B. & Likens, G.E. (2009) Adaptive monitoring: a new paradigm for long-term research and monitoring. *Trends in Ecology and Evolution*, **24**(9), 482–486.
- MacKenzie, D.I., Nichols, J.D., Lachman, G.B., Droege, S., Andrew Royle, J. & Langtimm, C.A. (2002) Estimating site occupancy rates when detection probabilities are less than one. *Ecology*, **83**(8), 2248–2255. [https://doi.org/10.1890/0012-9658\(2002\)083\[2248:esorwd\]2.0.co;2](https://doi.org/10.1890/0012-9658(2002)083[2248:esorwd]2.0.co;2)
- Marolla, F., Aarvak, T., Øien, I.J., Mellard, J.P., Henden, J.-A., Hamel, S. et al. (2019) Assessing the effect of predator control on an endangered goose population subjected to predator-mediated food web dynamics. *Journal of Applied Ecology*, **56**(5), 1245–1255. <https://doi.org/10.1111/1365-2664.13346>
- Meerburg, B.G., Singleton, G.R. & Kijlstra, A. (2009) Rodent-borne diseases and their risks for public health. *Critical Reviews in Microbiology*, **35**(3), 221–270. <https://doi.org/10.1080/10408410902989837>
- Meerburg, B.G., Singleton, G.R. & Leirs, H. (2009) The year of the rat ends—time to fight hunger! *Pest Management Science*, **65**(4), 351–352. <https://doi.org/10.1002/ps.1718>
- Mölle, J.P., Kleiven, E.F., Ims, R.A. & Soininen, E.M. (2021) Using subnivean camera traps to study Arctic small mammal community dynamics during winter. *Arctic Science*, **8**, 1–17. <https://doi.org/10.1139/as-2021-0006>
- Nicolau, P.G., Sørbye, S.H. & Yoccoz, N.G. (2020) Incorporating capture heterogeneity in the estimation of autoregressive coefficients of animal population dynamics using capture–recapture data. *Ecology and Evolution*, **10**(23), 12710–12726. <https://doi.org/10.1002/ece3.6642>
- Nicolau, P.G., Sørbye, S.H., Yoccoz, N.G., & Ims, R.A. (in press) Seasonality, density dependence and spatial population synchrony. *Proceedings of the National Academy of Sciences*.

- Oli, M.K. (2019) Population cycles in voles and lemmings: state of the science and future directions. *Mammal Review*, **49**(3), 226–239. <https://doi.org/10.1111/mam.12156>
- Otis, D.L., Burnham, K.P., White, G.C. & Anderson, D.R. (1978) Statistical inference from capture data on closed animal populations. *Wildlife Monographs*, 3–135 ISSN 00840173, 19385455.
- Øvrejorde, A. Calibrating abundance indices of small rodents in subarctic tundra. MSci thesis, Univ. of Tromsø, 2007.
- Palencia, P., Rowcliffe, J.M., Vicente, J. & Acevedo, P. (2021) Assessing the camera trap methodologies used to estimate density of unmarked populations. *Journal of Applied Ecology*, **58**(8), 1583–1592. <https://doi.org/10.1111/1365-2664.13913>
- Palmer, M.S., Swanson, A., Kosmala, M., Arnold, T. & Packer, C. (2018) Evaluating relative abundance indices for terrestrial herbivores from large-scale camera trap surveys. *African Journal of Ecology*, **56**(4), 791–803. <https://doi.org/10.1111/aje.12566>
- Parsons, M.A., Orloff, A.E. & Prugh, L.R. (2021) Evaluating livetrapping and camera-based indices of small-mammal density. *Canadian Journal of Zoology*, **99**(6), 521–530. <https://doi.org/10.1139/cjz-2020-0298>
- Powell, R.A. & Proulx, G. (2003) Trapping and marking terrestrial mammals for research: integrating ethics, performance criteria, techniques, and common sense. *ILAR Journal*, **44**(4), 259–276. <https://doi.org/10.1093/ilar.44.4.259>
- Rendall, A.R., Sutherland, D.R., Cooke, R. & White, J. (2014) Camera trapping: a contemporary approach to monitoring invasive rodents in high conservation priority ecosystems. *PLoS ONE*, **9**(3), e86592. <https://doi.org/10.1371/journal.pone.0086592>
- Rota, C.T., Ferreira, M.A.R., Kays, R.W., Forrester, T.D., Kalies, E.L., McShea, W.J. et al. (2016) A multispecies occupancy model for two or more interacting species. *Methods in Ecology and Evolution*, **7**(10), 1164–1173. <https://doi.org/10.1111/2041-210X.12587>
- Simpson, D., Rue, H., Riebler, A., Martins, T.G. & Sørbye, S.H. (2017) Penalising model component complexity: a principled, practical approach to constructing priors. *Statistical Science*, **232**(1), 1–28. <https://doi.org/10.1214/16-STS576>
- Soininen, E.M., Henden, J.-A., Ravolainen, V.T., Yoccoz, N.G., Bråthen, K.A., Killengreen, S.T. et al. (2018) Transferability of biotic interactions: temporal consistency of arctic plant–rodent relationships is poor. *Ecology and Evolution*, **8**(19), 9697–9711. <https://doi.org/10.1002/ece3.4399>
- Soininen, E.M., Jensvoll, I., Killengreen, S.T. & Ims, R.A. (2015) Under the snow: a new camera trap opens the white box of subnivean ecology. *Remote Sensing in Ecology and Conservation*, **1**(1), 29–38. <https://doi.org/10.1002/rse2.2>
- Stenseth, N.C. (1999) Population cycles in voles and lemmings: density dependence and phase dependence in a stochastic world. *Oikos*, **87**(3), 427. <https://doi.org/10.2307/3546809>
- Tast, J. (1966) The root vole, *Microtus oeconomus* (Pallas), as an inhabitant of seasonally flooded land. *Annales Zoologici Fennici*, **3**(3), 127–171.
- Turchin, P., Oksanen, L., Ekerholm, P., Oksanen, T. & Henttonen, H. (2000) Are lemmings prey or predators? *Nature*, **405**(6786), 562–565. <https://doi.org/10.1038/35014595>
- Turchin, P. & Hanski, I. (2001) Contrasting alternative hypotheses about rodent cycles by translating them into parameterized models. *Ecology Letters*, **4**(3), 267–276. <https://doi.org/10.1046/j.1461-0248.2001.00204.x>
- Villette, P., Krebs, C.J., Jung, T.S. & Boonstra, R. (2015) Can camera trapping provide accurate estimates of small mammal (*Myodes rutilus* and *Peromyscus maniculatus*) density in the boreal forest? *Journal of Mammalogy*, **97**(1), 32–40. <https://doi.org/10.1093/jmammal/gyv150>
- Wearn, O.R. & Glover-Kapfer, P. (2019) Snap happy: camera traps are an effective sampling tool when compared with alternative methods. *Royal Society Open Science*, **6**(3), 181748. <https://doi.org/10.1098/rsos.181748>
- Wiens, J.A. (1989) Spatial scaling in ecology. *Functional Ecology*, **3**(4), 385–397.
- Wilson, D.E. & Reeder, D.A.M. (2005) *Mammal species of the world: a taxonomic and geographic reference*, Vol. 2. Baltimore, MD: Johns Hopkins University Press.
- Yoccoz, N.G. & Ims, R.A. (2004) Spatial population dynamics of small mammals: some methodological and practical issues. *Animal Biodiversity and Conservation*, **27**(1), 427–435.
- Yoccoz, N.G., Nichols, J.D. & Boulinier, T. (2001) Monitoring of biological diversity in space and time. *Trends in Ecology and Evolution*, **16**(8), 446–453. [https://doi.org/10.1016/S0169-5347\(01\)02205-4](https://doi.org/10.1016/S0169-5347(01)02205-4)

## Supporting Information

Additional supporting information may be found online in the Supporting Information section at the end of the article.

## Appendix S1